An *Anaplasma phagocytophilum* T4SS effector, AteA, is essential for tick infection.

Jason M. Park[1*], Brittany M. Genera[1], Deirdre Fahy[1], Kyle T. Swallow[1], Curtis M. Nelson[2], Jonathan D. Oliver[3], Dana K. Shaw[1], Ulrike G. Munderloh[2], Kelly A. Brayton[1]

[1]Program in Vector-borne Disease, Department of Veterinary Microbiology and Pathology, Washington State University, Pullman, WA, USA

[2]Department of Entomology, College of Food, Agricultural, and Natural Resource Sciences, University of Minnesota, Saint Paul, MN, USA.

[3]Division of Environmental Health Sciences, School of Public Health, University of Minnesota, Minneapolis, MN. USA

Corresponding Author: *Jason M. Park; Jason.Park@wsu.edu

Running title: An actin-targeting tick-specific effector

ABSTRACT

Pathogens must adapt to disparate environments in permissive host species, a feat that is especially pronounced for vector-borne microbes, which transition between vertebrate hosts and arthropod vectors to complete their lifecycles. Most knowledge about arthropod-vectored bacterial pathogens centers on their life in the mammalian host, where disease occurs. However, disease outbreaks are driven by the arthropod vectors. Adapting to the arthropod is critical for obligate intracellular rickettsial pathogens, as they depend on eukaryotic cells for survival. To manipulate the intracellular environment, these bacteria use Type IV Secretion Systems (T4SS) to deliver effectors into the host cell. To date, few rickettsial T4SS translocated effectors have been identified and have only been examined in the context of mammalian infection. We identified an effector from the tick-borne rickettsial pathogen *Anaplasma phagocytophilum*, HGE1_02492, as critical for survival in tick cells and acquisition by ticks *in vivo.* Conversely, HGE1_02492 was dispensable during mammalian cell culture and murine infection. We show HGE1_02492 is translocatable in a T4SS-dependent manner to the host cell cytosol. In eukaryotic cells, the HGE1_02492 localized with cortical actin filaments, which is dependent on multiple sub-domains of the protein. HGE1_02492 is the first arthropod-vector specific T4SS translocated effector identified from a rickettsial pathogen. Moreover, the subcellular target of HGE1_02492 suggests that *A. phagocytophilum* is manipulating actin to enable arthropod colonization. Based on these findings, we propose the name AteA for *Anaplasma* (*phagocytophilum*) tick effector A. Altogether, we show that *A. phagocytophilum* uses distinct strategies to cycle between mammals and arthropods.

39 Importance:

40 Ticks are the number one vector of pathogens for livestock worldwide and for humans in
41 the US. The biology of tick transmission is an understudied area. Understanding this critical
42 interaction could provide opportunities to affect the course of disease spread. In this study we
43 examined the zoonotic tick-borne agent *Anaplasma phagocytophilum* and identified a secreted
44 protein, AteA, that is expressed in a tick-specific manner. These secreted proteins, termed
45 effectors, are the first proteins to interact with the host environment. AteA is essential for
46 survival in ticks and appears to interact with cortical actin. Most effector proteins are studied in
47 the context of the mammalian host; however, understanding how this unique set of proteins
48 affect tick transmission is critical to developing interventions.

49

INTRODUCTION

Multi-host pathogens often have specific adaptation mechanisms to survive in disparate environments (1). For example, vector-borne microbes must adapt and survive in both vertebrate hosts and arthropod vectors (2). These two environments differ significantly with discrepancies in body temperature, nutrient availability, cell types infected, physiological architecture, and immunological pressures (2). Most of our understanding of tick-borne pathogens focuses on interactions with mammalian hosts, as this is where disease occurs. However, the mammal represents only half of the lifecycle for tick borne pathogens. In contrast, little is known about how tick-vectored pathogens mediate interactions with the arthropod. With over 680 million years of evolution separating ticks from mammals (3), our understanding of mammal-pathogen interactions cannot simply be transposed onto ticks (2).

Adapting to different environments is especially critical for obligate intracellular rickettsial pathogens, which are intimately dependent on both arthropod and vertebrate host cells. One of the most common tick-borne rickettsial human pathogens in the United States is *Anaplasma phagocytophilum*, which causes human granulocytic anaplasmosis (4). To complete its lifecycle, *A. phagocytophilum* must transit between *Ixodes scapularis* ticks and mammalian hosts. Interestingly, *A. phagocytophilum* host cell tropisms are not equivalent between mammals and ticks. In mammals, the bacterium preferentially infects neutrophils. In contrast, *A. phagocytophilum* must infect and traverse the tick midgut, travel through the hemocoel, and infect the salivary glands of the arthropod (5, 6). Given the disparities in the host environment and cell tropisms, it is expected that *A. phagocytophilum* would have unique expression profiles adapted for each situation. Transcriptional studies demonstrated that *A. phagocytophilum* differentially transcribes 41% of its genes when growth in tick cells was compared to mammalian cells (7, 8). Transposon mutagenesis found many *A. phagocytophilum* genes are dispensable for growth in the human monocyte cell line HL60 (9), and several of these same

genes are upregulated during tick infection. Altogether, this suggests that the tick-specific genes may be involved in arthropod-pathogen interactions (7, 8).

Rickettsial pathogens primarily manipulate host cell biology through effector proteins that are delivered to the host cytosol with a Type 4 Secretion System (T4SS) (10, 11). T4SS effector molecules subvert host cell defenses and modulate a wide variety of host cell processes (12–19). A common target of such effectors can be the actin cytoskeleton, which forms the structural scaffolding of the host cell (20). When compared to the model intracellular bacterium *Legionella pneumophila* (1), relatively little is known about the effector repertoire from *A. phagocytophilum* and other rickettsial pathogens. Only five *A. phagocytophilum* T4SS translocated proteins have been identified to date, and none in the context of tick colonization (16, 17, 21–23). The machine learning algorithm OPT4e predicts that *A. phagocytophilum* encodes 48 candidate effectors (24). Fifteen of these candidate genes show unique expression patterns during mammalian and tick cell infection (7, 8). Putative effector HGE1_02492 (APH_0546 in *A. phagocytophilum* strain HZ) demonstrated the highest transcriptional increase when grown in tick cell culture, relative to mammalian cells. Herein, we show that HGE1_02492 is critical for growth in tick cells and colonization of ticks *in vivo*. Further, HGE1_02492 is deliverable by the T4SS into host cell cytosol, where it associates with cortical actin filaments, through multiple sub-domains of the protein. Based on our findings we propose the name AteA, for *A*naplasma (*phagocytophilum*) tick effector A, and will henceforth refer to HGE1_02492 as AteA. Altogether, we have identified and characterized the first arthropod-vector specific effector from *A. phagocytophilum*, which targets the eukaryotic cytoskeleton.

RESULTS

An protein of 1103 amino acids (~120 kD) is encoded by *ateA* (HGE1_02492) and appears to be unique to *A. phagocytophilum*. It has 100% sequence identity with APH_0546 from a different strain of *A. phagocytophilum,* strain HZ. *In silico* analysis of AteA predicts most of the protein is highly disordered, with an N-terminal globular domain (25) and there are two regions containing tandem repeats starting at amino acids 431 and 702 (26).

Expression of ateA is specific to growth in tick cells

Previous transcriptomics studies using tiling arrays demonstrated that *ateA* was upregulated during *A. phagocytophilum* culture in ISE6 tick cells, and was minimally expressed during growth in the human monocyte-like cell line HL60 (7, 8). Repetitive sequences, like those found in *ateA*, can artifactually inflate transcriptional signals in tiling arrays. We therefore used qRT-PCR with primers targeting non-repetitive sequences to quantify *ateA* expression patterns from *A. phagocytophilum* grown in HL60 and ISE6 cells. Housekeeping *A. phagocytophilum* genes, *rpoB* and *groEL*, are equally expressed when grown in either mammalian or tick cell lines (7, 27), and were therefore used as baseline controls for expression. Our findings demonstrate that *ateA* expression was >8 fold higher during growth in tick cells than in mammalian cells (Figure 1A).

A. phagocytophilum survival in tick cells is dependent on ateA expression

The tick-specific expression pattern of *ateA* led us to ask if it impacts growth in tick cells. For this experiment, we used several tools available to us, including an *ateA* insertion mutant that we previously isolated from a *A. phagocytophilum* Himar1 transposon mutant library (9). As a control strain, we used another mutant, which contains the Himar1 transposon in an intergenic location. This strain has been shown to be phenotypically equivalent to wild-type *A. phagocytophilum* (27, 28). Our analysis confirmed that transcription of *ateA* was abolished in the

ateA::Himar1 mutant, but transcription of housekeeping genes, *rpoB* and *groEL,* and the conserved *Anaplasma* gene encoding major surface protein 5, *msp5,* were all unaffected (Figure 1B). To test whether the *ateA*::Himar1 mutation impacted growth in the ISE6 cell line, both HL60 and ISE6 tick cells were infected with the *ateA*::Himar1 mutant and growth rates were compared to the intergenic transposon control strain. We found that *ateA*::Himar1 growth in HL60 cells was comparable to the control strain (Figure 1C), but *ateA*::Himar1 growth in ISE6 cells was significantly attenuated, indicating *ateA* is necessary for survival in tick cells (Figure 1D).

Expression of ateA is necessary for in vivo tick colonization

To examine the importance of *ateA in vivo,* we infected mice with either the control (intergenic transposon strain) or the *ateA*::Himar1 mutant strain. No colonization defect was observed in mice, indicating that *ateA* is dispensable during mammalian infection (Figure 2A). In contrast, larval *I. scapularis* ticks that fed to repletion on *A. phagocytophilum* burden-matched mice acquired significantly less of the *ateA*::Himar1 mutant when compared to the control. This indicates that *ateA* is critical for *A. phagocytophilum* colonization of the tick (Figure 2B).

AteA *is a T4SS substrate*

Several translocated effector prediction algorithms (OPT4e (24), S4TE (29), and T4EffPred (30)) predict that AteA is a T4SS substrate. To empirically test if AteA is translocatable by a T4SS, we used a well-established (31) surrogate assay in *Legionella pneumophila* (32). In this system, the candidate T4SS substrate is fused to adenylate cyclase (CyaA) and expressed in *L. pneumophila*. Candidate effector translocation is detected by accumulation of cAMP in host cells during *L. pneumophila* infection. CyaA-AteA led to significantly greater cAMP than the control (CyaA alone) (Figure 3A). Secretion was not

146 detected from the T4SS deficient *L. pneumophila* strain (*dotA*-), indicating translocation of AteA
147 is T4SS dependent.

148 A secretion signal common to many T4SS translocated proteins are charged residues at
149 the C-terminus (32, 33). We therefore removed 11 C-terminal amino acids from AteA or
150 mutagenized two acidic residues to basic residues in the C-terminus and tested secretion.
151 Neither manipulation strategy affected secretion (Figure 3B), indicating that a different feature of
152 AteA is being recognized by the T4SS. Intrinsically unstructured regions are another feature
153 common among translocated proteins (34). *In silico* analysis of AteA predicts most of the protein
154 is highly disordered, with only the N-terminal portion scoring for a globular structure (25) (Figure
155 3D). The disordered region has two prominent tandem repeat segments containing either 40 or
156 59 amino acid repeat units (26) (Figure 3E). We tested four large truncation fragments of CyaA-
157 AteA for translocation (Figure 3E). Truncations retaining a large relative amount of the
158 disordered region were secreted in our assay. The truncation that removed the disordered
159 region, leaving only the N-terminal globular region, was not translocated. Altogether, this
160 suggests that AteA contains multiple internal secretion signals, or that the unstructured nature of
161 the protein itself is being recognized by the T4SS for translocation (Figure 3C,E).

162 *AteA localizes to the cortical actin cytoskeleton and is dependent on multiple domains*

163 Since AteA is translocated to the host cell, we examined the eukaryotic host cell
164 structures that AteA may be targeting by ectopically expressing a GFP fusion protein (eGFP-
165 AteA) in HeLa cells. Laser-scanning confocal microscopy revealed that eGFP-AteA appeared as
166 branched filamentous structures, resembling the actin cytoskeleton (Figure 4). Filamentous
167 actin (F-actin) was visualized using fluorescently labeled Phalloidin, which revealed that AteA
168 co-localized with actin filaments (Figure 4). Many pathogens are known to target actin, which
169 alters host cell processes with the goal of promoting replication and survival. Two prominent F-
170 actin morphologies in cells are cortical actin and stress fibers. Cortical actin resembles a

branched web of fibers just under the cell surface. Stress fibers appear as linear actin bundles connecting two anchor points across the cell (35). The highly branched appearance of AteA localization led us to ask if it was associating with cortical actin. We therefore stained with Cortactin (cortical actin binding protein) and found co-localized with eGFP-AteA (Figure 5). The lack of AteA localization with longer linear actin fibers and the co-localization with Cortactin led us to conclude AteA preferentially associates with the cortical actin network.

To identify the portions of AteA responsible for localization to the actin cortex, truncations of the protein were constructed and ectopically expressed in HeLa cells (Figure 6). Removal of the C-terminal region following the repeat segments (eGFP-AteA aa1-918) did not change the localization pattern relative to the full-length protein (Figure 6B, C). Truncations that removed the second tandem repeat region (eGFP-AteA aa 1-574) reduced localization with Phalloidin and caused dispersed distribution following the topology of the cell surface (Figure 6D). The N-terminal globular domain alone (eGFP-AteA aa 1-266) showed a similar localization pattern to eGFP-AteA aa 1-574 (Figure 6E). These results suggested that the second tandem repeat region (residues 703-918) is necessary for localization with actin. When this region is removed the protein appears to associate with the cell's cortex. To test how the other regions of AteA impact the localization we performed the converse experiment, expressing truncations beginning at the N-terminus. AteA lacking the globular N-terminal region (eGFP-AteA aa 251-2094) lost preference for the cell's cortex, but retained association with actin fibers. This indicates that the N-terminal region of AteA is necessary for the cortical localization (Figure 6F). Interestingly, the actin fibers associated with AteA lacking the N-terminal globular region did not resemble a cortical actin morphology, but appeared more branch-like or distorted than typical actin stress fibers (Figure 6F). Truncations that removed the central region of AteA containing the first set of tandem repeats (eGFP-AteA aa 558-1094) resulted in the loss of the branched pattern altogether. Instead, the protein localized with long linear actin fibers characteristic of

196 stress fibers (Figure 6G). The C-terminal portion of AteA alone (eGFP-AteA aa 918-1094) did
197 not localize with Phalloidin and resembled eGPF alone (Figure 6H). Taken together our findings
198 indicate that the second tandem repeat region of AteA is responsible for localization to actin
199 fibers, the central region of the protein alters this actin localization pattern, and the N-terminal
200 domain provides specificity to the cortex. Altogether, these regions function in combination to
201 associate AteA with actin at the cell cortex.

202 **DISCUSSION**

203 Here we demonstrate the *A. phagocytophilum* gene encoding *ateA* is highly expressed
204 in the tick environment, is essential for growth and survival within tick cells, and is a T4SS
205 translocated substrate that targets the eukaryotic cytoskeleton. Further, *ateA* is necessary for *A.*
206 *phagocytophilum* acquisition by *I. scapularis* larvae when feeding on an infected host. However,
207 *ateA* was dispensable for growth in mammalian cell culture, and mutation did not affect bacterial
208 burden in mice. To our knowledge, this is the first description of an arthropod specific rickettsial
209 T4SS translocated effector.

210 AteA joins the few T4SS effectors identified from *A. phagocytophilum* (16, 17, 21–23).
211 However, machine learning algorithms predict *A. phagocytophilum* encodes many more that
212 remain to be tested (24). Among the 48 putative effectors predicted by OPT4e, fifteen are
213 differentially transcribed between mammalian and tick cells (7, 8). The three best characterized
214 *A. phagocytophilum* T4SS translocated effectors, Ats-1 (17), AnkA (15, 16), and HGE14 (23),
215 are all downregulated during growth in tick cells (7, 8), suggesting their contributions may be
216 more important during mammalian infection. Our understanding of how *A. phagocytophilum*
217 mediates interactions within mammalian cells is limited, but even less is understood about how
218 the bacteria navigate tick cell biology. A full mechanistic understanding of how rickettsial
219 pathogens facilitate their vector-borne life cycle will require effector identification and
220 characterization in the context of both mammalian hosts and arthropod vectors.

While genetic tools among rickettsial organisms remain limited (36), the *A. phagocytophilum* transposon mutant library (9) allowed us to isolate and test a mutation disrupting *ateA*. Although maintenance of the library in HL60 cell culture precludes mutation of genes essential for mammalian infection, it has equipped us to test the contributions of genes that are important for growth in the tick. This is the second mutant from these libraries shown to have a tick cell specific phenotype. Mutation of an outer-membrane O-methyltransferase similarly led to a tick cell specific infection defect (28). Additionally, transposon mutation of a paralogous T4SS component, *virB6-4,* partially attenuated growth in both tick and mammalian cells demonstrating this mutant collection also retains some utility for investigating incomplete phenotypes in mammalian cell models (27). We took the *ateA*::Himar1 mutant beyond cell culture experiments and demonstrated an *in vivo* phenotype through both murine and tick infections that *ateA* is important for bacterial acquisition by ticks from a blood meal. Our work with *ateA*::Himar1 represents the first *A. phagocytophilum* mutant examined in live ticks.

Due to the difficulties of generating recombinant expression systems in an obligate intracellular bacterium (36), efficient T4SS translocation assays using rickettsial organisms have not yet been developed. However surrogate systems in *Legionella* (31)*, Coxiella* (23)*,* and *Escherichia* (17, 37) have been used to identify rickettsial T4SS substrates. We demonstrated that *L. pneumophila* recognizes and translocates AteA into the host cell cytosol in a T4SS dependent manner. Motifs at the C-terminus often serve as translocation signals for both the *Legionella* and rickettsial T4SS, but they are not universally required and alternative signals can be used (32, 33). AteA contains multiple charged residues in the C-terminus that we determined are dispensable for translocation. Instead, the large, disordered region of AteA was sufficient for translocation. This suggests that the T4SS is recognizing the unstructured nature of the protein or unidentified internal secretion signals. Indeed, disordered regions are a common characteristic among bacterial effectors (34). While the specificity of the *Legionella* T4SS

translocation assay cannot be directly projected onto the *A. phagocytophilum* T4SS, *A. phagocytophilum* effectors Ats1, AnkA, and HGE14 also contain intrinsically disordered regions suggesting that this may be a common feature recognized for T4SS translocation (25).

Intracellular bacteria exist among the scaffold of the host cell's cytoskeleton composed of actin, tubulin, and various intermediate filaments. Pathogens manipulate this cytoskeleton network to promote internalization, evade destruction, alter intracellular trafficking, and disseminate within and between cells (20). Our understanding of how *A. phagocytophilum* interfaces with this cellular scaffold is limited, but differences exist between mammalian and tick cell infection (38, 39). During mammalian infection the *A. phagocytophilum* vacuole protein AptA recruits intermediate filaments to the *Anaplasma* vacuole. However, transcription of *aptA* is not detectable during *A. phagocytophilum* infection in ticks (39). Actin polymerization is necessary for *A. phagocytophilum* entry into mammalian cells, but during tick cell infection actin is phosphorylated and depolymerized, which is not seen during mammalian infection (38). Although ectopic expression of AteA did not appear to lead to actin depolymerization, this possibility will require further study. We found that AteA localized with branched actin at the cell cortex and was dependent on the predicted tandem repeats and the N-terminal globular domain (Figure 6). Many other intracellular pathogens are known to manipulate cortical actin to attach to the host cell, induce internalization of the bacteria (20, 40), alter endosome maturation (41, 42), block degradation by the lysosome (43), support the pathogen containing vacuole (44), induce extrusion from the host cell (45), and mediate cell to cell bacterial transfer (20, 46). Understanding how AteA manipulates the cytoskeleton to further the *A. phagocytophilum* infection cycle will require further mechanistic dissection.

We demonstrated that *A. phagocytophilum ateA* is specifically important in the tick environment. While examination of AteA localization in tick cells is desired, ectopic expression in ISE6 cells is difficult as transfection efficiency is extremely low, and we were unable to

visualize AteA in tick cells. However, we were able to visualize AteA localization with cortical actin in mammalian cells, which may have been possible because actin is one of the most conserved proteins across all eukaryotes (47). Further, mammalian systems have previously been used to investigate multiple actin targeting T4SS effectors, despite mammals not being the evolutionarily relevant environment (1, 41, 42, 48, 49). The tick-specific expression of *ateA* is highlighted by its dispensability during mammalian infection, and severe attenuation of the knockout during tick infection. Why *A. phagocytophilum* requires *ateA* during tick infection remains unclear, but it may stem from the different cell types infected. In mammals the bacteria preferentially infect phagocytic neutrophils, while in ticks it infects multiple non-phagocytic cell types. AteA may be required to induce internalization or trafficking within tick cells, that neutrophils perform without manipulation.

In summary we have identified the first tick-specific translocated effector from *A. phagocytophilum* and have shown that it targets cortical actin. While most research on *A. phagocytophilum* focuses on mammalian infection, it is increasingly clear that the mammalian and tick environments are not equivalent. Given that the arthropod vector is the driver of *A. phagocytophilum* transmission, it is critical to understand how these bacteria survive in the tick. We expect that *A. phagocytophilum* deploys a unique repertoire of effectors to navigate the tick environment, with *ateA* being only the first of many to identify.

Materials and Methods

Bacterial and Eukaryotic cell culture

Escherichia coli was grown using solid and liquid lysogeny broth (LB) medium with the addition of kanamycin or zeocin 25 µg ml^{-1} antibiotics for selection as needed. *L. pneumophila* Lp02 and Lp03 (dotA−) strains were cultured using N-(2-acetamido)-2-aminoethanesulfonic acid (ACES) buffered yeast extract medium (AYE) and solid charcoal buffered yeast extract agar

medium (CYE). *L. pneumophila* cultures were supplemented with 0.4 mg ml^{-1} iron(III) nitrate, 0.135 mg ml^{-1} cysteine (50), 0.1 mg ml^{-1} thymidine, and when appropriate 50 µg ml^{-1} Kanamycin.

HeLa human cervical epithelial cells (American Type Culture Collection [ATCC]; CCL-2) cells were maintained in Eagle's Minimum Essential Medium (MEM; Corning; 10-010-CV) with 10% fetal bovine serum (FBS: Atlanta biologicals: S11550) and 1× Glutamax (Gibco; 35050061). HL60 human promyelocytic cells (ATCC; CCL-240) and the THP1 human monocyte cell line (ATCC TIB-202) were maintained in Roswell Park Memorial Institute (RPMI) 1640 medium with 10% FBS and 1× Glutamax. Mammalian cell cultures were maintained in a humidified chamber at 37°C with 5% CO_2. HL60 density was kept between 5×10^4 and 1×10^6 and limited to less than 20 passages to prevent differentiation or phenotypic drift.

A. phagocytophilum strain HGE1 and mutant lines were cultured in HL60 cells(9). Insertion mutant *ateA*::Himar1 and control strain were isolated from a previously reported *A. phagocytophilum* Himar1 transposon mutant library (9). The control strain contains the Himar1 transposon in an intergenic location, and has been shown to be phenotypically equivalent to wild-type (27, 28). Infection status of HL60 cells was assessed by Diff-Quick Romanowsky–Giemsa staining. *A. phagocytophilum* were liberated from HL60 cells by 27-gauge needle syringe lysis to generate host-cell-free organisms. Bacterial numbers were estimated as previously described (51, 52).

Tick cells derived from embryonated eggs of the blacklegged tick, *I. scapularis* (Say), ISE6, were grown in L15C-300 medium with 10% FBS (Sigma; F0926), 10% tryptone phosphate broth (TPB; BD; B260300) and 0.1% lipoprotein cholesterol concentrate (MP Biomedicals; 219147680)(53). Infected ISE6 cell cultures were additionally supplemented with 0.25% $NaHCO_3$ and 25 mM HEPES buffer (Sigma). Tick cell cultures were incubated at 34°C and 1% CO_2 (6).

319 *Anaplasma phagocytophilum* growth curves

320 Growth of *A. phagocytophilum* strains in HL60 and ISE6 cells were evaluated similar to
321 previously described (27, 28). Briefly HL60 cells were seeded at $5x10^4$ cells per well of 24 well
322 plates. The plate was then infected with $5x10^4$ host cell-free *A. phagocytophilum* per well for an
323 MOI of 1. Triplicate wells were harvested at the time of inoculation and 1, 2, 3, 4, and 5 days
324 post inoculation. ISE6 cells were seeded at $3x10^5$ cells per well of 24 well plates and allowed to
325 adhere to the plate overnight. Host cell-free preparations of *A. phagocytophilum* strains were
326 prepared immediately before inoculation and bacteria were suspended in L15C300
327 supplemented with 0.25% NaHCO3 and 25 mM HEPES. ISE6 plates were inoculated at $3x10^6$
328 *A. phagocytophilum* per well for an MOI of 10. Twenty-four hours post infection the tick cell
329 media was exchanged for fresh L15C300 +NaHCO3 +HEPES to remove remaining extracellular
330 bacteria, and three wells were collected for initial timepoint. Triplicate samples were collected at
331 subsequent time points and frozen to be processed for gDNA using a QIAGEN DNAeasy blood
332 and tissue kit. Change in bacteria and host cell gDNA copies was assessed by qPCR using iTaq
333 universal SYBR green Supermix (Bio-Rad; 1725125) in duplicate reactions. Bacterial gDNA was
334 measured targeting the single copy *A. phagocytophilum* gene *msp5*. HL60 and ISE6 host cell
335 gDNA was measured targeting genes *tlr9* (toll-like receptor 9) and *crt* (calreticulin). Respectively
336 (27) (Table S1).

337 *Transcriptional analysis of ateA*

338 Triplicate samples were collected during the HL60 and ISE6 *A. phagocytophilum* growth
339 curve experiments. Samples were processed to purify RNA using Direct-zol RNA micro-prep kit®
340 (ZymoResearch) according to product protocols for tissue culture samples. The Verso cDNA
341 Synthesis Kit (ThermoFisher) was used to generate cDNA. Transcripts of *ateA*, *rpoB, groEL*,
342 and *msp5* genes were measured by qPCR using iTaq universal SYBR green Supermix (Bio-

Rad; 1725125) according to Bio-Rad specified cycle conditions. Transcription of *ateA* was compared between experimental groups by ΔΔCt using *rpoB* as the housekeeping control gene.

Animal infection

Two gender matched groups of ten, 6-week-old C57BL/6 mice (The Jackson Laboratory) were intraperitoneally infected with either the *ateA*::Himar1 mutant or the control strain at 1×10^7 host cell-free *A. phagocytophilum* bacteria per mouse. The control strain contains the Himar1 transposon in an intergenic location, and has been shown to be phenotypically equivalent to wild-type (27, 28). Seven days post infection 25-50 µl of blood was collected from the lateral saphenous vein. Levels of *A. phagocytophilum* in the blood was measured by qPCR (16S rRNA relative to mouse *β-actin* (51, 54)) (Table S1). Uninfected *I. scapularis* larval ticks were purchased from Oklahoma State University (Stillwater, OK, USA). Ticks were housed at 23°C with 16/8-h light/dark photoperiods in 95 - 100% humidity. As sources of tick acquisition for *A. phagocytophilum*, two burden-matched-pairs of mice were selected from the *ateA*::Himar1 and control strain infected mice. Each mouse was individually housed and infested with 200 naïve unfed *I. scapularis* larvae. Three to seven days post infestation replete larvae were collected, individually flash frozen with liquid nitrogen, ground with a pestle, dissolved in TRIzol® and processed to purify total RNA according to Direct-zol RNA micro-prep kit® protocol. The Verso cDNA Synthesis Kit (ThermoFisher) was used to generate cDNA. Levels of viable *A. phagocytophilum* in the ticks were measured by quantifying *A. phagocytophilum* 16S rRNA relative to *I. scapularis β-actin* transcripts by qRT-PCR (Table S1) by absolute quantification (51, 54). All animal use protocols were approved by the Washington State University Institutional Animal Care and Use Committee (ASAF #6630). The animals were housed and maintained in an AAALAC-accredited facility at Washington State University in Pullman, WA.

Plasmid Construction

Full length and truncations of the *ateA* open reading frame were amplified from *A. phagocytophilum* genomic DNA with Gateway® compatible primers (Table S1). Amplicons were introduced into pDONR/Zeo by BP Clonase® (Invitrogen). Sequence confirmed inserts were then transferred to destination expression vectors with LR Clonase® (Invitrogen). For ectopic expression in mammalian cells, we used a Gateway® compatible version of pEGFP-C1 (Clontech), pEZYegfp (Addgene). To create a Gateway® destination vector for use in translocation assays (pJC125DEST), the Gateway® attR cassette was inserted into the CyaA translational fusion construct pJC125 (55) at a *SmaI* restriction site. CyaA fusion constructs were introduced to *L. pneumophila* by electroporation.

Translocation Assay

THP-1 cells were seeded at 5 x10^5/mL in 24 well plate and differentiated to macrophage-like cells by treatment with 200 nM Phorbol 12-myristate 13-acetate (PMA; Sigma) for 18 hrs. Transformed *L. pneumophila* cells were grown overnight to an OD_{600} of 2.0, at which point the bacteria were in post-exponential phase, highly motile, and infectious. Expression of the CyaA fusion proteins was induced by adding 1 mM IPTG for 1 hour, and motility was verified by microscopy of wet mounted samples. Cell culture medium was used to dilute *L. pneumophila* which was then used to infect THP-1 cells at an MOI of 1. One hour post infection, cAMP was extracted and quantified as previously described (56) using the cAMP Parameter Assay Kit (R&D Systems).

Immunofluorescence

HeLa cells were transfected using FuGENE® 6 Transfection Reagent at a 3:1 FuGENE to DNA ratio. Proteins were expressed for 36 – 48 hrs, then fixed in 4% paraformaldehyde. Fixed cells were permeabilized with 0.1% Triton X-100 for 15 min and washed three times in PBS. Cells were incubated with Alexa Fluor™ 568 Phalloidin (Thermo Fisher Scientific) in PBS

containing 1% bovine serum albumin (BSA) for 30 min. Cells were washed three times for five minutes with PBS and coverslips were mounted on slides using Vectashield® mounting medium with DAPI. Slides were imaged using a Leica SP8 confocal microscope.

Statistics

All *in vitro* experiments were performed with three biological replicates, measured in technical duplicate assays, and experiments were repeated three times to ensure reproducibility of findings. *In vivo* experiments used ten independently inoculated mice per group. 17-20 ticks were collected per mouse. Two burden matched mice pairs were used for experimental replicates of the tick feeding. Data were expressed as means and graphed with standard deviation. Data points were analyzed with a Student T-test (Mann-Whitney) for *in vitro* experiments and *in vivo* experiments were analyzed with an unpaired Welch's T-test. Statistical analysis was performed and graphed with GraphPad Prism version 9.0. A P-value of <0.05 was considered statistically significant.

406 **REFERENCES**

407 1. Park JM, Ghosh S, O'Connor TJ. 2020. Combinatorial selection in amoebal hosts drives
408 the evolution of the human pathogen *Legionella pneumophila*. 4. Nature Microbiology
409 5:599–609.

410 2. Park JM, Oliva Chávez AS, Shaw DK. 2021. Ticks: More Than Just a Pathogen Delivery
411 Service. Frontiers in Cellular and Infection Microbiology 11.

412 3. Kumar S, Stecher G, Suleski M, Hedges SB. 2017. TimeTree: A Resource for Timelines,
413 Timetrees, and Divergence Times. Molecular Biology and Evolution 34:1812–1819.

414 4. Eisen RJ, Kugeler KJ, Eisen L, Beard CB, Paddock CD. 2017. Tick-Borne Zoonoses in the
415 United States: Persistent and Emerging Threats to Human Health. ILAR J 58:319–335.

416 5. Ueti MW, Reagan JO, Knowles DP, Scoles GA, Shkap V, Palmer GH. 2007. Identification
417 of Midgut and Salivary Glands as Specific and Distinct Barriers to Efficient Tick-Borne
418 Transmission of *Anaplasma marginale*. Infection and Immunity 75:2959–2964.

419 6. Munderloh UG, Jauron SD, Fingerle V, Leitritz L, Hayes SF, Hautman JM, Nelson CM,
420 Huberty BW, Kurtti TJ, Ahlstrand GG, Greig B, Mellencamp MA, Goodman JL. 1999.
421 Invasion and Intracellular Development of the Human Granulocytic Ehrlichiosis Agent in
422 Tick Cell Culture. Journal of Clinical Microbiology 37:2518–2524.

423 7. Nelson CM, Herron MJ, Felsheim RF, Schloeder BR, Grindle SM, Chavez AO, Kurtti TJ,
424 Munderloh UG. 2008. Whole genome transcription profiling of *Anaplasma*
425 *phagocytophilum* in human and tick host cells by tiling array analysis. BMC Genomics 9:1–
426 16.

427 8. Nelson CM, Herron MJ, Wang X-R, Baldridge GD, Oliver JD, Munderloh UG. 2020. Global
428 Transcription Profiles of *Anaplasma phagocytophilum* at Key Stages of Infection in Tick
429 and Human Cell Lines and Granulocytes. Frontiers in Veterinary Science 7:111.

430 9. O'Conor MC, Herron MJ, Nelson CM, Barbet AF, Crosby FL, Burkhardt NY, Price LD,
431 Brayton KA, Kurtti TJ, Munderloh UG. 2021. Biostatistical prediction of genes essential for
432 growth of *Anaplasma phagocytophilum* in a human promyelocytic cell line using a random
433 transposon mutant library. Pathogens and Disease 79:ftab029.

434 10. Gillespie JJ, Phan IQH, Driscoll TP, Guillotte ML, Lehman SS, Rennoll-Bankert KE,
435 Subramanian S, Beier-Sexton M, Myler PJ, Rahman MS, Azad AF. 2016. The *Rickettsia*
436 type IV secretion system: unrealized complexity mired by gene family expansion.
437 Pathogens and Diseases 74.

438 11. Gillespie JJ, Brayton KA, Williams KP, Diaz MAQ, Brown WC, Azad AF, Sobral BW. 2010.
439 Phylogenomics Reveals a Diverse Rickettsiales Type IV Secretion System. Infection and
440 Immunity 78:1809–1823.

441 12. Beyer A, Truchan H, Levi M, Walker N, Borjesson D, Carlyon J. 2014. The *Anaplasma*
442 *phagocytophilum* effector AmpA hijacks host cell SUMOylation. Cellular Microbiology 17.

443 13. Lehman SS, Noriea NF, Aistleitner K, Clark TR, Dooley CA, Nair V, Kaur SJ, Rahman MS,
444 Gillespie JJ, Azad AF, Hackstadt T. 2018. The Rickettsial Ankyrin Repeat Protein 2 Is a
445 Type IV Secreted Effector That Associates with the Endoplasmic Reticulum. mBio
446 9:e00975-18.

447 14. Voss OH, Gillespie JJ, Lehman SS, Rennoll SA, Beier-Sexton M, Rahman MS, Azad AF.
448 2020. Risk1, a Phosphatidylinositol 3-Kinase Effector, Promotes *Rickettsia typhi*
449 Intracellular Survival. mBio 11.

15. Garcia-Garcia JC, Rennoll-Bankert KE, Pelly S, Milstone AM, Dumler JS. 2009. Silencing of Host Cell CYBB Gene Expression by the Nuclear Effector AnkA of the Intracellular Pathogen *Anaplasma phagocytophilum*. Infection and Immunity 77:2385–2391.

16. Lin M, Dulk-Ras AD, Hooykaas PJJ, Rikihisa Y. 2007. *Anaplasma phagocytophilum* AnkA secreted by type IV secretion system is tyrosine phosphorylated by Abl-1 to facilitate infection. Cellular Microbiology 9:2644–2657.

17. Niu H, Kozjak-Pavlovic V, Rudel T, Rikihisa Y. 2010. *Anaplasma phagocytophilum* Ats-1 Is Imported into Host Cell Mitochondria and Interferes with Apoptosis Induction. PLOS Pathogens 6:e1000774.

18. Yan Q, Zhang W, Lin M, Teymournejad O, Budachetri K, Lakritz J, Rikihisa Y. 2021. Iron robbery by intracellular pathogen via bacterial effector–induced ferritinophagy. PNAS 118.

19. Lin M, Liu H, Xiong Q, Niu H, Cheng Z, Yamamoto A, Rikihisa Y. 2016. *Ehrlichia* secretes Etf-1 to induce autophagy and capture nutrients for its growth through RAB5 and class III phosphatidylinositol 3-kinase. Autophagy 12:2145–2166.

20. Colonne PM, Winchell CG, Voth DE. 2016. Hijacking Host Cell Highways: Manipulation of the Host Actin Cytoskeleton by Obligate Intracellular Bacterial Pathogens. Frontiers in Cellular and Infection Microbiology 6:107.

21. Tang H, Zhu J, Wu S, Niu H. 2020. Identification and characterization of an actin filament-associated *Anaplasma phagocytophilum* protein. Microbial Pathogenesis 147:104439.

22. Zhu J, He M, Xu W, Li Y, Huang R, Wu S, Niu H. 2019. Development of TEM-1 β-lactamase based protein translocation assay for identification of *Anaplasma phagocytophilum* type IV secretion system effector proteins. 1. Science Reports 9:4235.

472 23. Sinclair SHG, Garcia-Garcia JC, Dumler JS. 2015. Bioinformatic and mass spectrometry
473 identification of *Anaplasma phagocytophilum* proteins translocated into host cell nuclei.
474 Frontiers in Microbiology 6:55.

475 24. Esna Ashari Z, Brayton KA, Broschat SL. 2019. Prediction of T4SS Effector Proteins for
476 *Anaplasma phagocytophilum* Using OPT4e, A New Software Tool. Front Microbiol 10.

477 25. Erdős G, Pajkos M, Dosztányi Z. 2021. IUPred3: prediction of protein disorder enhanced
478 with unambiguous experimental annotation and visualization of evolutionary conservation.
479 Nucleic Acids Research 49:W297–W303.

480 26. Newman AM, Cooper JB. 2007. XSTREAM: A practical algorithm for identification and
481 architecture modeling of tandem repeats in protein sequences. BMC Bioinformatics 8:382.

482 27. Crosby FL, Munderloh UG, Nelson CM, Herron MJ, Lundgren AM, Xiao Y-P, Allred DR,
483 Barbet AF. Disruption of VirB6 Paralogs in *Anaplasma phagocytophilum* Attenuates Its
484 Growth. Journal of Bacteriology 202:e00301-20.

485 28. Oliva Chávez AS, Fairman JW, Felsheim RF, Nelson CM, Herron MJ, Higgins L, Burkhardt
486 NY, Oliver JD, Markowski TW, Kurtti TJ, Edwards TE, Munderloh UG. 2015. An O-
487 Methyltransferase Is Required for Infection of Tick Cells by *Anaplasma phagocytophilum*.
488 PLoS Pathog 11:e1005248.

489 29. Noroy C, Lefrançois T, Meyer DF. 2019. Searching algorithm for Type IV effector proteins
490 (S4TE) 2.0: Improved tools for Type IV effector prediction, analysis and comparison in
491 proteobacteria. PLoS Computational Biology 15:e1006847.

492 30. Zou L, Nan C, Hu F. 2013. Accurate prediction of bacterial type IV secreted effectors using
493 amino acid composition and PSSM profiles. Bioinformatics 29:3135–3142.

494 31. Lockwood S, Voth DE, Brayton KA, Beare PA, Brown WC, Heinzen RA, Broschat SL.
495 2011. Identification of *Anaplasma marginale* type IV secretion system effector proteins.
496 PLoS One 6:e27724.

497 32. Huang L, Boyd D, Amyot WM, Hempstead AD, Luo Z-Q, O'Connor TJ, Chen C, Machner
498 M, Montminy T, Isberg RR. 2011. The E Block motif is associated with *Legionella*
499 *pneumophila* translocated substrates. Cellular Microbiology 13:227–245.

500 33. Christie PJ, Whitaker N, González-Rivera C. 2014. Mechanism and structure of the
501 bacterial type IV secretion systems. Biochimica et Biophysica Acta (BBA) - Molecular Cell
502 Research 1843:1578–1591.

503 34. Marín M, Uversky VN, Ott T. 2013. Intrinsic Disorder in Pathogen Effectors: Protein
504 Flexibility as an Evolutionary Hallmark in a Molecular Arms Race. Plant Cell 25:3153–
505 3157.

506 35. Chalut KJ, Paluch EK. 2016. The Actin Cortex: A Bridge between Cell Shape and
507 Function. Developmental Cell 38:571–573.

508 36. McClure EE, Chávez ASO, Shaw DK, Carlyon JA, Ganta RR, Noh SM, Wood DO, Bavoil
509 PM, Brayton KA, Martinez JJ, McBride JW, Valdivia RH, Munderloh UG, Pedra JHF. 2017.
510 Engineering of obligate intracellular bacteria: progress, challenges and paradigms. Nature
511 Reviews Microbiology 15:544–558.

512 37. Whitaker N, Berry TM, Rosenthal N, Gordon JE, Gonzalez-Rivera C, Sheehan KB,
513 Truchan HK, VieBrock L, Newton ILG, Carlyon JA, Christie PJ. 2016. Chimeric Coupling
514 Proteins Mediate Transfer of Heterologous Type IV Effectors through the *Escherichia coli*
515 pKM101-Encoded Conjugation Machine. Journal of Bacteriology 198:2701–2718.

516 38. Sultana H, Neelakanta G, Kantor FS, Malawista SE, Fish D, Montgomery RR, Fikrig E.
517 2010. *Anaplasma phagocytophilum* induces actin phosphorylation to selectively regulate
518 gene transcription in Ixodes scapularis ticks. Journal of Experimental Medicine 207:1727–
519 1743.

520 39. Sukumaran B, Mastronunzio JE, Narasimhan S, Fankhauser S, Uchil PD, Levy R, Graham
521 M, Colpitts TM, Lesser CF, Fikrig E. 2011. *Anaplasma phagocytophilum* AptA modulates
522 Erk1/2 signalling. Cellular Microbiology 13:47–61.

523 40. Hardt W-D, Chen L-M, Schuebel KE, Bustelo XR, Galán JE. 1998. *S. typhimurium*
524 Encodes an Activator of Rho GTPases that Induces Membrane Ruffling and Nuclear
525 Responses in Host Cells. Cell 93:815–826.

526 41. Michard C, Sperandio D, Baïlo N, Pizarro-Cerdá J, LeClaire L, Chadeau-Argaud E,
527 Pombo-Grégoire I, Hervet E, Vianney A, Gilbert C, Faure M, Cossart P, Doublet P. 2015.
528 The *Legionella* Kinase LegK2 Targets the ARP2/3 Complex To Inhibit Actin Nucleation on
529 Phagosomes and Allow Bacterial Evasion of the Late Endocytic Pathway. mBio 6.

530 42. Hervet E, Charpentier X, Vianney A, Lazzaroni J-C, Gilbert C, Atlan D, Doublet P. 2011.
531 Protein Kinase LegK2 Is a Type IV Secretion System Effector Involved in Endoplasmic
532 Reticulum Recruitment and Intracellular Replication of *Legionella pneumophila*. Infection
533 and Immunity 79:1936–1950.

534 43. Walpole GFW, Plumb JD, Chung D, Tang B, Boulay B, Osborne DG, Piotrowski JT, Catz
535 SD, Billadeau DD, Grinstein S, Jaumouillé V. 2020. Inactivation of Rho GTPases by
536 *Burkholderia* cenocepacia Induces a WASH-Mediated Actin Polymerization that Delays
537 Phagosome Maturation. Cell Reports 31:107721.

538 44. Kumar Y, Valdivia RH. 2008. Actin and intermediate filaments stabilize the *Chlamydia*
539 *trachomatis* vacuole by forming dynamic structural scaffolds. Cell Host Microbe 4:159–169.

540 45. Thomas S, Popov VL, Walker DH. 2010. Exit Mechanisms of the Intracellular Bacterium
541 Ehrlichia. PLoS One 5:e15775.

542 46. Lamason RL, Welch MD. 2017. Actin-based motility and cell-to-cell spread of bacterial
543 pathogens. Current Opinion in Microbiology 35:48–57.

544 47. Wickstead B, Gull K. 2011. The evolution of the cytoskeleton. Journal of Cell Biology
545 194:513–525.

546 48. He L, Lin Y, Ge Z, He S, Zhao B, Shen D, He J, Lu Y. 2019. The *Legionella pneumophila*
547 effector WipA disrupts host F-actin polymerisation by hijacking phosphotyrosine signalling.
548 Cellular Microbiology 21:e13014.

549 49. Liu Y, Zhu W, Tan Y, Nakayasu ES, Staiger CJ, Luo Z-Q. 2017. A *Legionella* Effector
550 Disrupts Host Cytoskeletal Structure by Cleaving Actin. PLoS Pathogens 13:e1006186.

551 50. Feeley JC, Gibson RJ, Gorman GW, Langford NC, Rasheed JK, Mackel DC, Baine WB.
552 1979. Charcoal-yeast extract agar: primary isolation medium for *Legionella pneumophila*.
553 Journal of Clinical Microbiology 10:437–441.

554 51. Shaw DK, Wang X, Brown LJ, Chávez ASO, Reif KE, Smith AA, Scott AJ, McClure EE,
555 Boradia VM, Hammond HL, Sundberg EJ, Snyder GA, Liu L, DePonte K, Villar M, Ueti
556 MW, de la Fuente J, Ernst RK, Pal U, Fikrig E, Pedra JHF. 2017. Infection-derived lipids
557 elicit an immune deficiency circuit in arthropods. Nature Communications 8:14401.

558 52. Chen G, Wang X, Severo MS, Sakhon OS, Sohail M, Brown LJ, Sircar M, Snyder GA,
559 Sundberg EJ, Ulland TK, Olivier AK, Andersen JF, Zhou Y, Shi G-P, Sutterwala FS,

560 Kotsyfakis M, Pedra JHF. 2014. The Tick Salivary Protein Sialostatin L2 Inhibits Caspase-
561 1-Mediated Inflammation during *Anaplasma phagocytophilum* Infection. Infection and
562 Immunity 82:2553–2564.

563 53. Oliver JD, Chávez ASO, Felsheim RF, Kurtti TJ, Munderloh UG. 2015. An *Ixodes*
564 *scapularis* cell line with a predominantly neuron-like phenotype. Experimental and Applied
565 Acarology 66:427–442.

566 54. Sidak-Loftis LC, Rosche KL, Pence N, Ujczo JK, Hurtado J, Fisk EA, Goodman AG, Noh
567 SM, Peters JW, Shaw DK. 2022. The Unfolded-Protein Response Triggers the Arthropod
568 Immune Deficiency Pathway. mBio 0:e00703-22.

569 55. Myeni S, Child R, Ng TW, Kupko JJ, Wehrly TD, Porcella SF, Knodler LA, Celli J. 2013.
570 *Brucella* modulates secretory trafficking via multiple type IV secretion effector proteins.
571 PLoS Pathogens 9:e1003556.

572 56. Voth DE, Howe D, Beare PA, Vogel JP, Unsworth N, Samuel JE, Heinzen RA. 2009. The
573 *Coxiella burnetii* Ankyrin Repeat Domain-Containing Protein Family Is Heterogeneous, with
574 C-Terminal Truncations That Influence Dot/Icm-Mediated Secretion. Journal of
575 Bacteriology 191:4232–4242.

576
577

FIGURE LEGENDS

Figure 1. *ateA* is essential for *A. phagocytophilum* survival in tick cells, but dispensable within human cells. A) *A. phagocytophilum* gene expression during growth within tick ISE6 and human HL60 cells. Transcription of *ateA,* and housekeeping genes *rpoB* and *groEL*. B) Transcriptional analysis from *A. phagocytophilum* transposon mutants with the insertion site in a neutral intergenic location (control), or within the *ateA* gene, during culture of with tick ISE6 cells. Transcription measured by qRT-PCR of *ateA, msp5, rpoB,* and *groEL.* Transcription normalized to *rpoB.* Results shown are the mean of three biological replicates with two technical replicates each ± SD. *, P<0.05 (Student T-test). C,D) Growth of *A. phagocytophilum ateA* or control strain in C) human HL60 cells and D) tick ISE6 cells. Bacterial burden was measured as *Anaplasma* gDNA vs host cell gDNA via qPCR. Graphs are representative of three experimental replicates. Data shown are the mean of three biological replicates with two technical replicates each ± SD and is representative of three experimental replicates. *, < 0.05 (Mann Whitney T-test).

Figure 2. *ateA* is dispensable for murine infection, but mutation attenuates tick acquisition. A) *Anaplasma* burden in mouse blood 7 days post infection by intraperitoneal inoculation with $1x10^8$ host cell free *A. phagocytophilum ateA*::Himar1 or control. Blood samples were processed for DNA isolation and bacterial burden was measured by qPCR of *A. phagocytophilum* 16S rDNA relative to mouse actin by ΔΔCt. Each strain was tested in 5 male (squares) and 5 female (circles) mice and samples were tested in duplicate. Mice used for tick feeding are indicated by blue and green symbols. Blue symbols indicate experimental replicate 1. Green symbols indicate experimental replicate 2. B) *Ixodes scapularis* larvae were infected by feeding to repletion on *A. phagocytophilum* burden-matched mice infected. Whole replete *I. scapularis* larvae were processed for RNA. Bacterial loads were measured by *A. phagocytophilum* 16S

603 rRNA levels relative to mouse actin via qRT-PCR. Data shown represents ticks from two burden
604 matched mouse pairings indicated in blue and green for two experimental replicates. Blue
605 symbols indicate experimental replicate 1. Green symbols indicate experimental replicate 2. 17-
606 20 individual ticks were collected from each mouse as biological replicates, and each qRT-PCR
607 was performed in duplicate. **, < 0.005 (Welsh's T-test).

608 **Figure 3.** AteA is recognized and secreted by a T4SS. A, B, C) THP-1 cells were infected with a
609 *L. pneumophila* strain expressing the indicated Cya-fusion proteins for 1 hour. cAMP
610 concentrations were quantified from infected cell lysates by ELISA and compared as fold
611 change over CyaA alone. A) CyaA and CyaA-AteA expressed in both wild type *L. pneumophila*
612 Lp02 or T4SS-deficient Lp03 strain (T4SS -). B) C-terminal mutants of CyaA-AteA were
613 expressed in Lp02 and compared to CyaA alone and CyaA-AteA. C) Truncation constructs of
614 CyaA-AteA diagrammed in E were expressed in Lp02 and compared to CyaA alone and CyaA-
615 AteA. D) IUPred3 order/disorder plot of AteA protein. E) Diagram of AteA truncation mutants.
616 Tandem repeat regions highlighted. A, B, C) Error bars represent ± SD of the mean of three
617 biological replicates with two technical replicates each, and graph is representative of two
618 repeated experiments. *, < 0.05 (Mann Whitney T-test).

619 **Figure 4.** AteA localizes with F-actin. Confocal images of HeLa cells transiently transfected to
620 express eGFP or eGFP-AteA. Actin was stained with Alexa-fluor™ 564 Phalloidin 36 hrs post
621 transfection.

622 **Figure 5.** AteA localizes to cortical actin. Confocal images of HeLa cells transiently transfected
623 to express eGFP or eGFP-AteA. Cells were stained to visualize Cortactin at 36 hrs post
624 transfection.

625 **Figure 6.** Multiple regions of AteA influence localization with cortical actin. A - H) Left:
626 Schematic of eGFP-AteA fusion constructs and truncations used in transfections. A - H) Right:

627 Confocal images of HeLa cells transiently transfected to express eGFP, eGFP-AteA, or an
628 eGFP-AteA truncation construct as diagramed (Left). Cells were stained to visualize actin using
629 Alexa-fluor™ 564 Phalloidin at 36-48 hrs post transfection.

630

631 **ACKNOWLEDGEMENTS**

632 We are grateful to Daniel Voth at the University of Arkansas College of Medicine (Little Rock,
633 AR) and Jean Celli at Washington State University Paul G. Allen School for Global Health
634 (Pullman, WA) for sharing protocols and plasmids constructs for the CyaA secretion assay.
635 Tamara O'Connor at Johns Hopkins University (Baltimore, MD) generously provided *L.*
636 *pneumophila* Lp02 and Lp03 (*dotA*⁻) strains. Lisa Price and Nicole Burkhardt at the University of
637 Minnesota (Saint Paul, MN) for their assistance in isolating and verifying strains from the Himar1
638 transposon collection.

639 **FUNDING**

640 This work was funded through generous support from the National Institutes of Health (NIAID),
641 grant numbers R21AI154023, R21AI151412 to KAB, and R01AI042792. BMG was supported by
642 NIH training grant T32-GM008336.

643 **AUTHOR CONTRIBUTIONS**

644 **Jason M. Park:** Conceptualization, Methodology, Investigation, Writing - Original Draft &
645 Editing, Visualization, Funding acquisition. **Brittany M. Genera:** Methodology, Investigation,
646 Visualization, Reviewing & Editing. **Deirdre Fahy:** Methodology, Investigation, Review &
647 Editing. **Kyle T. Swallow:** Investigation. **Curtis M. Nelson and Jonathan D. Oliver:**
648 Investigation, Resources. **Dana K. Shaw:** Methodology, Investigation, Review & Editing. **Ulrike**

649 **G. Munderloh:** Resources, Funding acquisition. **Kelly A. Brayton:** Conceptualization,

650 Supervision, Funding acquisition, Review & Editing.

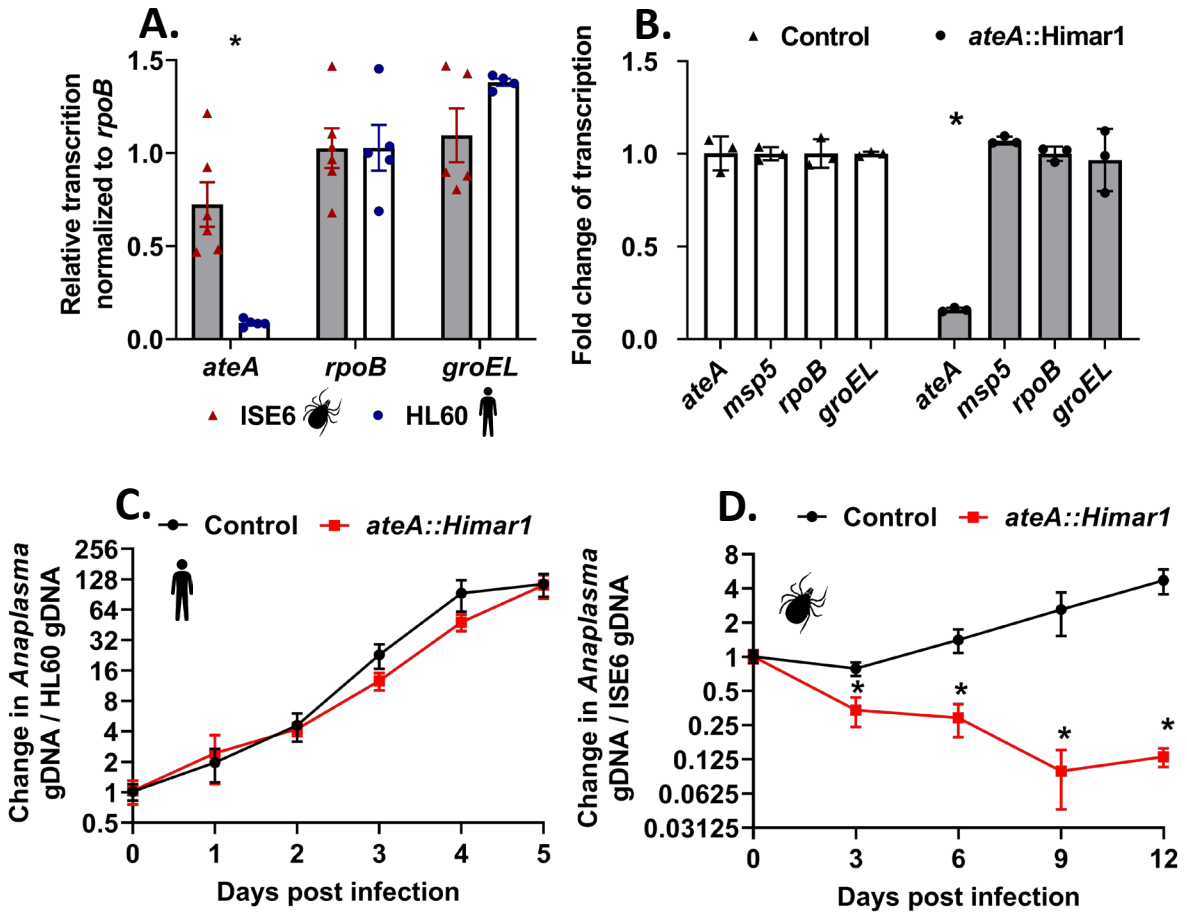

Figure 1. *ateA* is essential for *A. phagocytophilum* survival in tick cells, but dispensable within human cells.

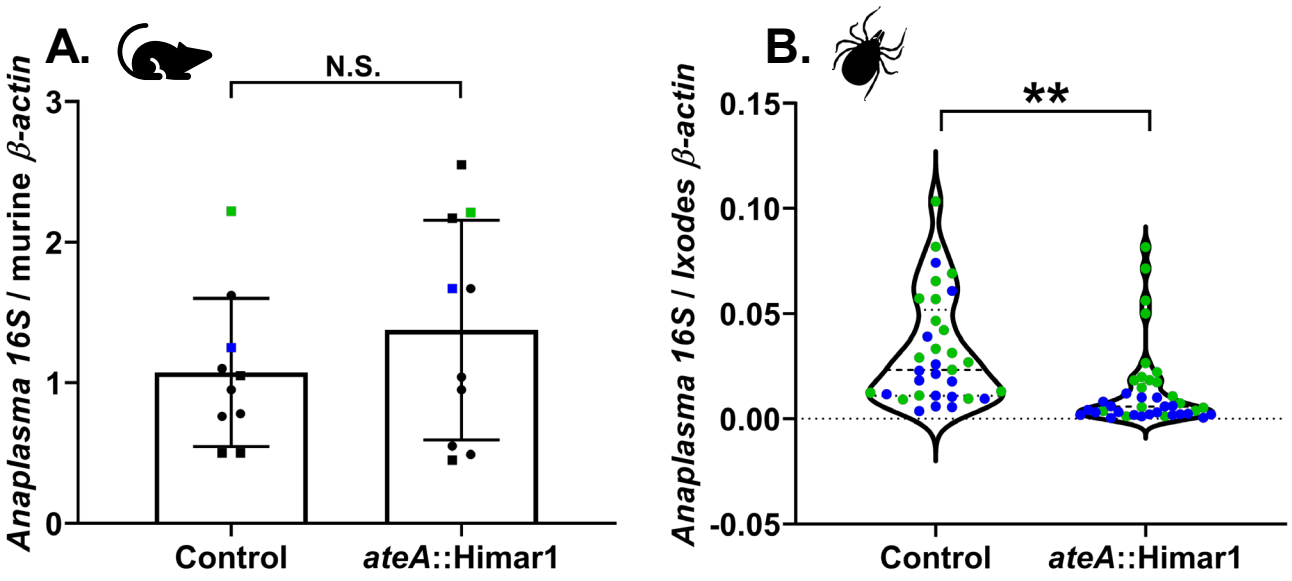

Figure 2. *ateA* is dispensable for murine infection, but mutation attenuates tick acquisition

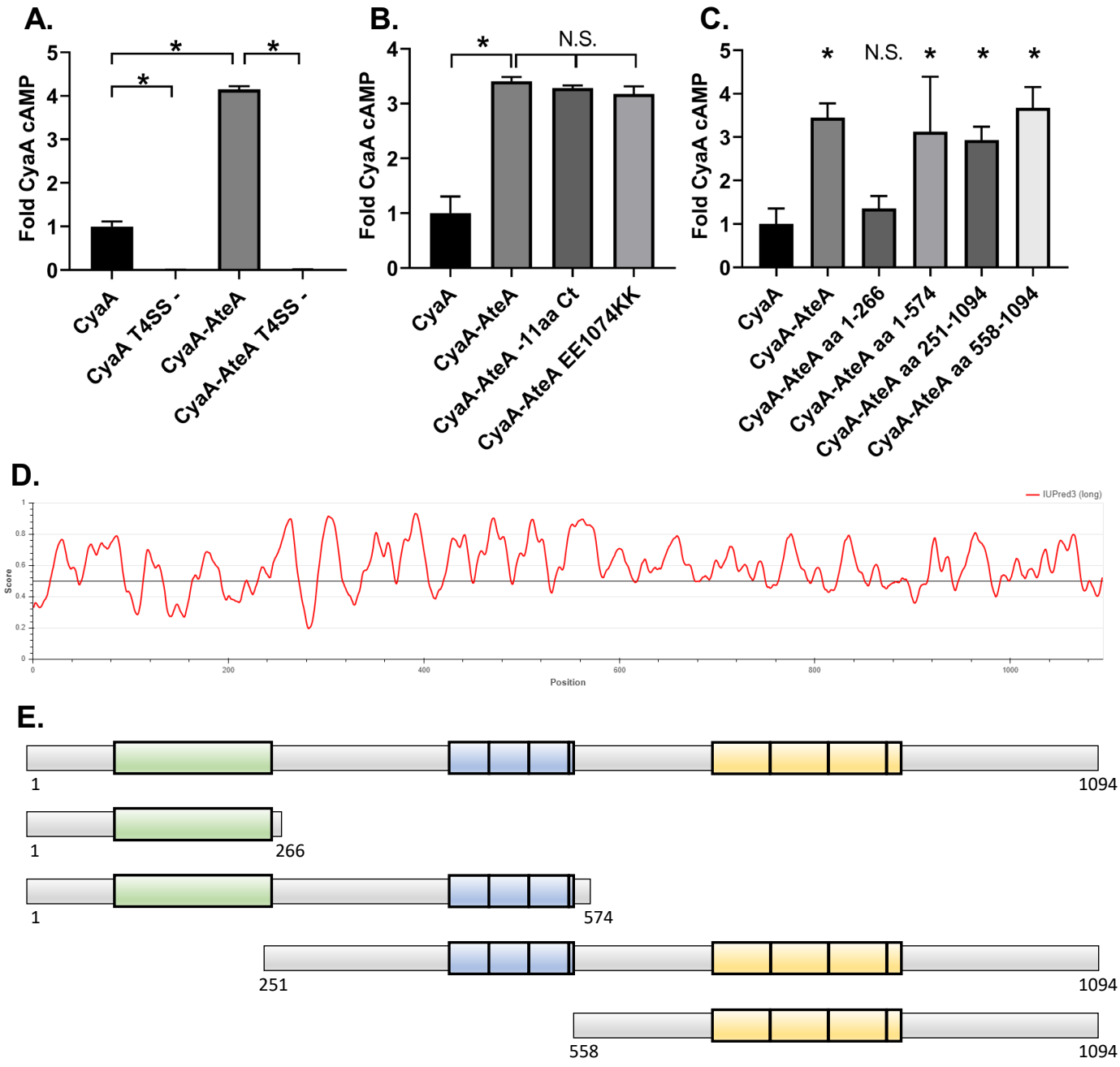

Figure 3. AteA is recognized and secreted by a T4SS.

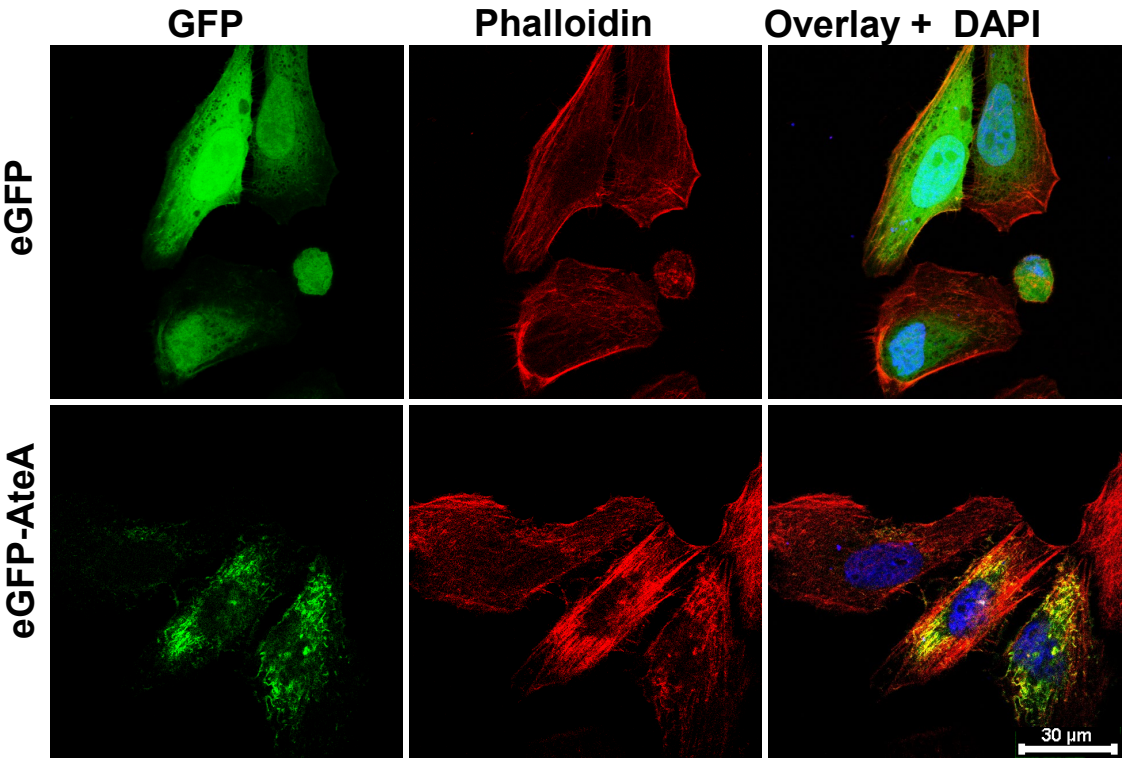

Figure 4. AteA localizes with F-actin.

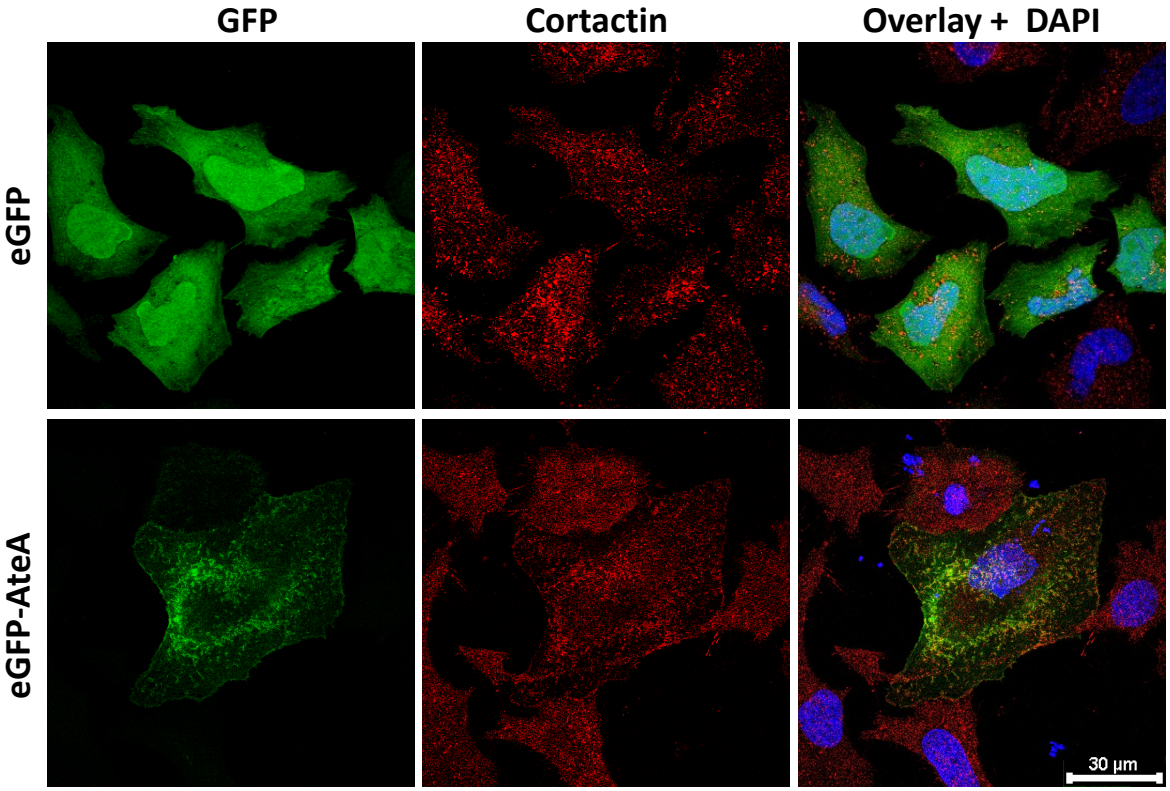

Figure 5. AteA localizes to cortical actin.

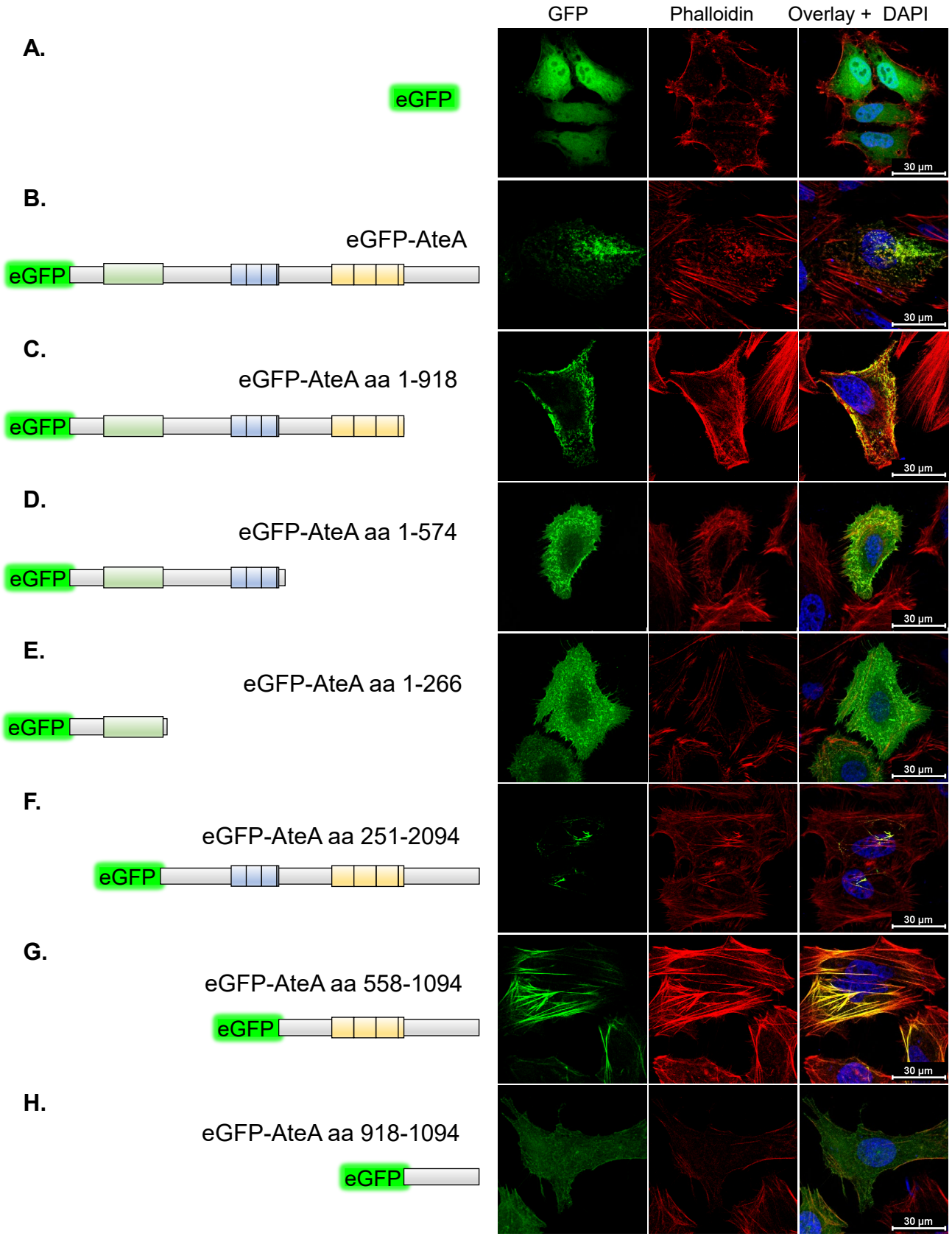

Figure 6. Multiple regions of AteA influence localization with cortical actin.

Supplemental Table 1.

Name	SEQ	Purpose
msp5 RT-qPCR F	TGCGGAACTTGGTATGGTATC	Quantify msp5 transcripts
msp5 RT-qPCR R	CTCATTTAACCTTTCAACAGTGTCA	
groEL F	AGGGAGGTAGTACGCATCCTAGA	Quantify groEL transcripts
groEL R	TGTGATCTCTGGCGACCCATAA	
rpoB F	GGCCTATGGTGCTGCTTATAC	Quantify rpoB transcripts
rpoB R	CCACACTCGAAGTTGCTATCC	
2492 qPCR F	GGCCTTGCTGCTTCCATAACC	qPCR of HGE1_2492 primers
2492 qPCR R	CTCTGTAGAAGGTGTTGCGTCTTC	
2492 at 570502 F	TTGCTAAGGGTGCGCCAAAG	Test purity of the HGE1_02492::Himar1 mutant
02492 at 570502 R	TTGGGTTCGGGATGGGTAGTAG	
msp5 qPCR F	AGATGCTGACTGGGGATGAG	quantification of msp5 Ap DNA
msp5 qPCR R	TCGGCATCAACCAAGTACAA	
crt ISE6 F	GTCAAGTCCGGCACAATCT	quantification of crt gene in ISE6 DNA
crt ISE6 R	CATCTTCTTCTCGGCATCCTT	
tlr9 F	CCCAGTCTTGGACTCAGAATTAG	quantification of tlr9 gene in HL60 DNA
tlr9 R	GGTATAGCCAGGGATTGGTTAAG	
Ap 16S-FL_F	TCCTGGCTCAGAACGAACG	Amplify full Ap 16s for qPCR standard
Ap 16S-FL_R	GTCACTGACCCAACCTTAAATGG	
M.m. B-actin_qPCR-R	ACGCGGGAGGAAGAGGATGCGGCAGTG	Quantify mouse actin transcripts
M.m. B-actin_qPCR-F	ACGCAGAGGGAAATCGTGCGTGAC	
Ap16s_qPCR-F	CCCTAAGGCCTTCCTCACTC	Quantify Anaplasma burdon in mouse blood
Ap16s_qPCR-R	CAGCCACACTGGAACTGAGA	
ISE6 actin full R	TACTGTAAAAACAATTTTTATTCCACCAATGAAG	Amplify ISE6 actin for qPCR standard.
ISE6 Actin Full F	ATTTCTTTACCATATTTGGAAGTACGCCACG	
I.s. actin_qPCR-F3	GCCGGGACCTTACAGACTATC	Quantify Ixodes scapularis tick actin primers
I.s. actin_qPCR-R3	CACGGACAATTTCACGCTCG	
Ap16s_qPCR-tick F	AAGCACTCCGCCTGGGGACT	Quantify Anaplasma burdon in ticks
Ap16s_qPCR-tick R	CCATGTCAAGGAGTGGTAAGG	
ChUp & out	ATTATCTTCCTCTCCCTTGCTGACC	PCR and sequencing outward from Himar1 transposon
HGE1_02492 F	GGGGACAAGTTTGTACAAAAAAGCAGGCTTAATGGGAAAATTAACAAAAATC	Gateway compatable HGE1_02492 cloning primers
HGE1_02492 R With Stop	GGGGACCACTTTGTACAAGAAAGCTGGGTACTAGAAACGTGCCCTTGATG	
2492_EE1074KK_F	GAATTAGCAAAACAACTTAAGAAAGGAGGAGTTCTTACGCAAGTGCTTGC	Site directed primers to reverse HGE1_02492 C-terminal charges
2492_EE1074KK_R	GCGTAAGAACTCCTCCTTTCTTAAGTTGTTTTGCTAATTCATGTACAGAT	
2492-11aa C-term GW_R	GGGGACCACTTTGTACAAGAAAGCTGGGTATTAAAGCACTTGCGTAAGAACTCCTCC	Clone HGE1_02492 removing 11aa from the C-teriminus
2492 aa 251-1094 F	GGGGACAAGTTTGTACAAAAAAGCAGGCTTAAGCGCTTCTAAGCACGATGG	Clone HGE1_02492 fragments into pDONR via gateway
2492 aa 558-1094 F	GGGGACAAGTTTGTACAAAAAAGCAGGCTTAAGTATGCTGACAAACAAACCTACTAC	Clone HGE1_02492 fragments into pDONR via gateway
2492 aa 1-266 R	GGGGACCACTTTGTACAAGAAAGCTGGGTACTACTGCTTATTAGAGGAATTAGACTC	Clone HGE1_02492 fragments into pDONR via gateway
2492 aa 1-574 R	GGGGACCACTTTGTACAAGAAAGCTGGGTACTAGTTTTTCAAAGATTTGGGTTCGGG	Clone HGE1_02492 fragments into pDONR via gateway
2492 918 C-term GW F	GGGGACAAGTTTGTACAAAAAAGCAGGCTTAAGTAACAGTGAGATTAAAAGCAAGTC	Clone HGE1_02492 fragments into pDONR via gateway
2492 aa918 stopCterm GW	GGGGACCACTTTGTACAAGAAAGCTGGGTACTAAGACTTGCTTTTAATCTCACTGTTA	Clone HGE1_02492 fragments into pDONR via gateway
2492 5' rev	GCTTCCGCAGAATCATTAGATTGCGGG	sequence from HGE1_02492 into vector
2492 3' F	GTGCAAGCACTACAACAAGAAAGGC	
peGFP C1 seq	CATGGTCCTGCTGGAGTTCGTG	sequencing pEGFP C1
2492 int F	CTCAGGTTCAGTTACGGGTTCTG	internal sequencing primers
2492 int R	AGCTCAATAGAAGTAGTAGGCTTGC	